separations

Article

Effective and Low-Cost Adsorption Procedure for Removing Chemical Oxygen Demand from Wastewater Using Chemically Activated Carbon Derived from Rice Husk

Wael I. Mortada [1,*], Raed A. Mohamed [2], Amir A. Abdel Monem [2], Marwa M. Awad [2] and Asaad F. Hassan [3]

[1] Urology and Nephrology Center, Mansoura University, Mansoura 35516, Egypt
[2] Petrochemical Program, Chemistry Department, Faculty of Science, Mansoura University, Mansoura 35516, Egypt
[3] Department of Chemistry, Faculty of Science, University of Damanhour, Damanhour 22511, Egypt
* Correspondence: w.mortada@mans.edu.eg

Abstract: Wastewater treatment by adsorption onto activated carbon is effective because it has a variety of benefits. In this work, activated carbon prepared from rice husk by chemical activation using zinc chloride was utilized to reduce chemical oxygen demand from wastewater. The as-prepared activated carbon was characterized by scanning electron microscope, Fourier transform infrared spectroscopy and nitrogen adsorption/desorption analysis. The optimum conditions for maximum removal were achieved by studying the impact of various factors such as solution pH, sorbent dose, shaking time and temperature in batch mode. The results displayed that the optimum sorption conditions were achieved at pH of 3.0, sorbent dose of 0.1 g L^{-1}, shaking time of 100 min and at room temperature (25 °C). Based on the effect of temperature, the adsorption process is exothermic in nature. The results also implied that the isothermal data might be exceedingly elucidated by the Langmuir model. The maximum removal of chemical oxygen demand by the activated carbon was 45.9 mg g^{-1}. The kinetic studies showed that the adsorption process follows a pseudo-first order model. The findings suggested that activated carbon from rice husk may be used as inexpensive substitutes for commercial activated carbon in the treatment of wastewater for the removal of chemical oxygen demand.

Keywords: activated carbon; rice husk; adsorption; chemical oxygen demand

Citation: Mortada, W.I.; Mohamed, R.A.; Monem, A.A.A.; Awad, M.M.; Hassan, A.F. Effective and Low-Cost Adsorption Procedure for Removing Chemical Oxygen Demand from Wastewater Using Chemically Activated Carbon Derived from Rice Husk. *Separations* **2023**, *10*, 43. https://doi.org/10.3390/separations10010043

Academic Editor: Gavino Sanna

Received: 30 December 2022
Revised: 7 January 2023
Accepted: 9 January 2023
Published: 10 January 2023

Copyright: © 2023 by the authors. Licensee MDPI, Basel, Switzerland. This article is an open access article distributed under the terms and conditions of the Creative Commons Attribution (CC BY) license (https://creativecommons.org/licenses/by/4.0/).

1. Introduction

Wastewaters produced from different industries contain organic and inorganic contaminants in addition to other harmful substances. Each year, 3 to 10 billion gallons of untreated waste are liberated from sewage treatment plants [1]. As a result, treating such effluent to an environmentally acceptable level is critical from both an environmental and economic standpoint. The existing issues in wastewater treatment systems are caused by an increase in the contamination with harmful substances that are difficult to degrade biologically [2].

An essential parameter in residential wastewater is chemical oxygen demand (COD), which measures the amount of oxygen needed to oxidize organic molecules chemically [3]. High COD levels are a sign of organics in the wastewater, which can reduce the amount of dissolved oxygen in the water and have significant environmental effects [4]. Therefore, the COD test is frequently used to evaluate the effectiveness of water treatment plants [5].

For COD removal from industrial effluents, a variety of strategies have been considered [6]. These include electrocoagulation [7], chemical coagulation [8], adsorption [9], nanofiltration [10], ozonation [11] and reverse osmosis [12].

Research efforts are being carried out to develop effective and inexpensive wastewater treatment techniques [13]. Adsorption is a potential approach for removing several forms of contaminants from wastewater [14]. Low-cost adsorbents of various sources such as agriculture waste can be employed for the removal of pollutants from wastewater [15]. The elimination of different contaminants by adsorption onto activated carbon is widely investigated for the treatment of wastewater [16]. Activated carbon is a porous material with a relatively high surface area and can be obtained from various agriculture wastes [17]. It is widely used to remove toxic metal ions [18], dyes [19], pharmaceutical residue [20], dissolved organic carbon [21], pesticide [22], and inorganic anions [23] from wastewater. The utilization of activated carbon derived from agricultural waste represents an additional advantage in terms of recycling this waste to obtain effective materials [24].

Rice husk (RH) is a by-product of the rice milling industry. The yearly global RH production is around 100 million tones [25]. Farmers frequently dump RH into the environment through burning, which releases CO_2, a greenhouse gas. Furthermore, eliminating it in farms may result in the growth of germs in the soil [26]. As a result, the rice husk must be recycled by turning it into active elements that may be utilized for environmental objectives [27]. Due to the high cellulose and lignin content of rice husk, it can be used as an excellent source of carbons to produce activated carbon.

In this work, chemically activated carbon was prepared from rice husk for reduction in COD from wastewater. The effects of various experimental factors such as pH, amount of activated carbon, stirring time and temperature were studied and optimized to obtain the maximum adsorption.

2. Results and Discussion

2.1. Characterization of the Activated Carbon

The SEM images of the activated carbon are shown in Figure 1. The surface morphology of the activated carbon is a porous multilayer texture with distinct cracks and cavities which are responsible for the high surface area of the prepared activated carbon. The cavities on the surfaces appear to be the consequence of $ZnCl_2$ evaporating during carbonization, leaving the empty area that it had previously filled [28]. However, the surface is covered in numerous tiny pits, which suggest that carbon gasification occurred on the outside surface during carbonization [29]. TEM image of the activated carbon is shown in Figure 2. The TEM analysis is seen to clearly establish the amorphous structure's nature [30]. The particles of the prepared activated carbon appeared to be aggregated due to the presence of surface chemical functional groups. TEM showed that the particle size ranged from 20 to 35 nm.

The FTIR spectrum (Figure 3) was performed to qualitatively characterize the surface function groups of the native rice husk and the activated carbon.

The spectrum of the native rice husk exhibits a band at about 3433 cm^{-1}, which is due to the vibration stretching of OH groups. The band at 2923 cm^{-1} is due to the $-CH_3$ of lignin [31]. The peak at 2860 cm^{-1}, which corresponds to aliphatic C-H stretching, indicates the presence of alkane moieties [32]. The C=O stretching vibrations between 1655 and 1713 cm^{-1} indicate hemicelluloses and lignin aromatic groups [33]. The peak at 1082 cm^{-1} may be due to the stretching vibration of Si-O-Si [34]. The other peaks at 2860 cm^{-1}, 1653–1711 cm^{-1} and 1082 cm^{-1} are attributed to aliphatic C-H, C=O and Si-O-Si stretching vibrations, respectively [35]. After calcination, most of these peaks are maintained, which means that these functional groups could reside on the surface of the prepared activated carbon.

Nitrogen gas adsorption/desorption isotherms and the BJH plot are presented in Figure 4a for the prepared activated carbon. The adsorption isotherm curve is classified as type II based on IUPAC. The surface area, total pore volume, and average pore radius were found to be 813.5 (S_{BET}, $m^2\ g^{-1}$), 0.3354 (V_P, $cm^3\ g^{-1}$), and 1.007 ($\bar{r}$, nm), respectively. The investigated solid samples of the Type II adsorption isotherm revealed the formation of multiple layers of adsorbed nitrogen gas molecules after the first layer is formed. The high specific surface area of the formed activated sample is related to the effect of the chemically activating agent ($ZnCl_2$ solution) for the formation of porous solid material [36].

The hysteresis loop belongs to type H4, which is related to the mesoporous structure of pores (2–50 nm) [37]. The inserted BJH methodology curve indicates that there are two observable peaks located at nearly 1.0 and 5.0 nm, while that located at 1.0 nm is the preferential one, which means that mesoporosity is the overwhelm case. The nitrogen adsorption isotherm onto the native rice husk powder can be classified as type I (Figure 4b) according to IUPAC classification, which belongs to monolayer adsorption onto the microporous surface [38]. The calculated surface area, total pore volume, and pore radius were found to be 41.76 $m^2\ g^{-1}$, 0.01705 $cm^3\ g^{-1}$, and 0.8165 nm. The lower surface area and total pore volume of rice husk compared with that activated with zinc chloride as the chemical activation agent is related to the effect of zinc chloride at higher temperature to create new pores.

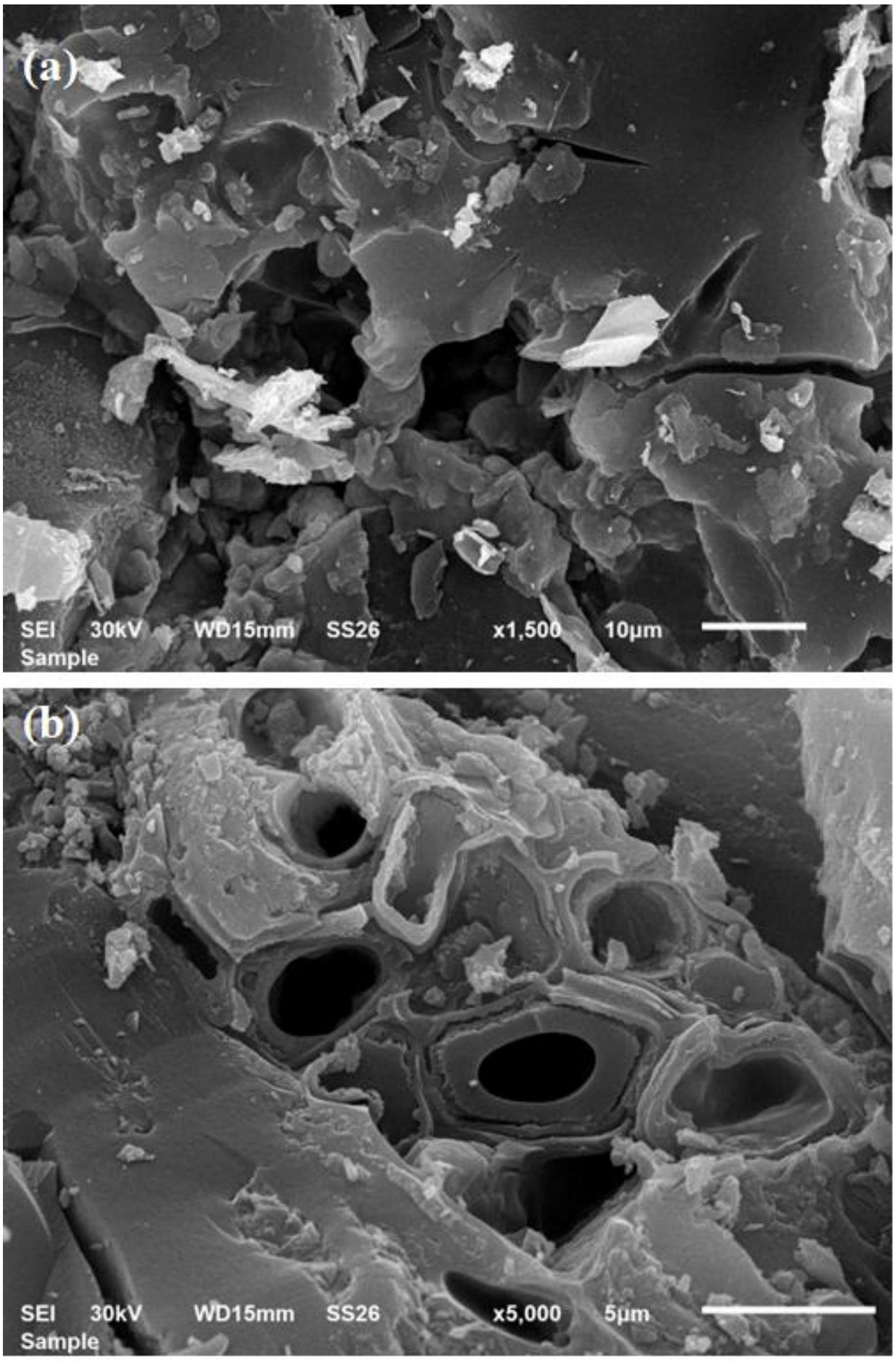

Figure 1. SEM images of the prepared activate carbon: (**a**) magnification 1500 (**b**) magnification 5000.

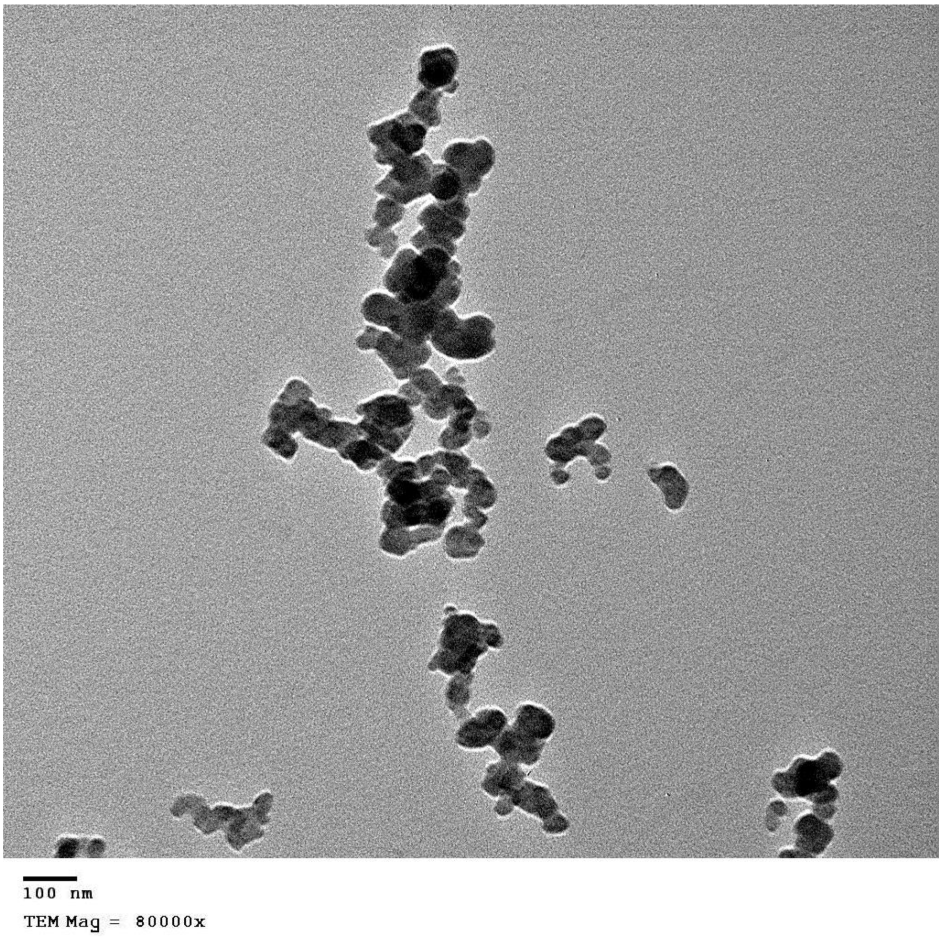

Figure 2. TEM image of the prepared activated carbon.

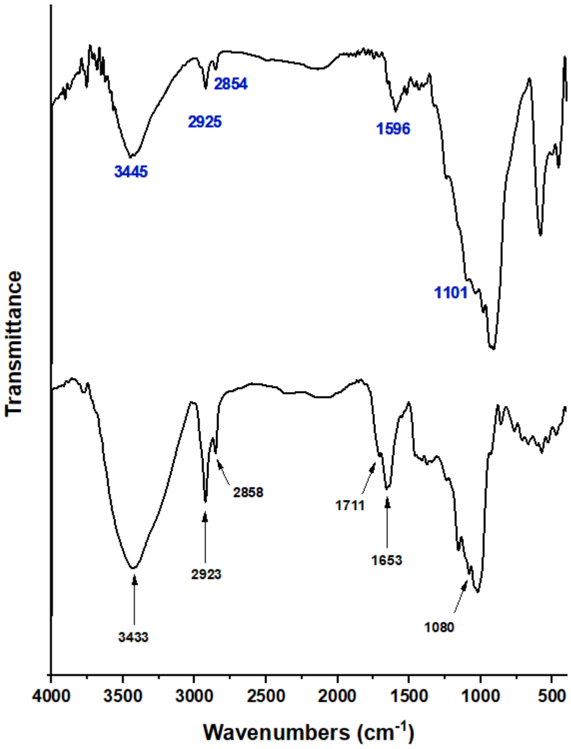

Figure 3. FT-IR spectrum of native rice husk and the activated carbon prepared from rice husk.

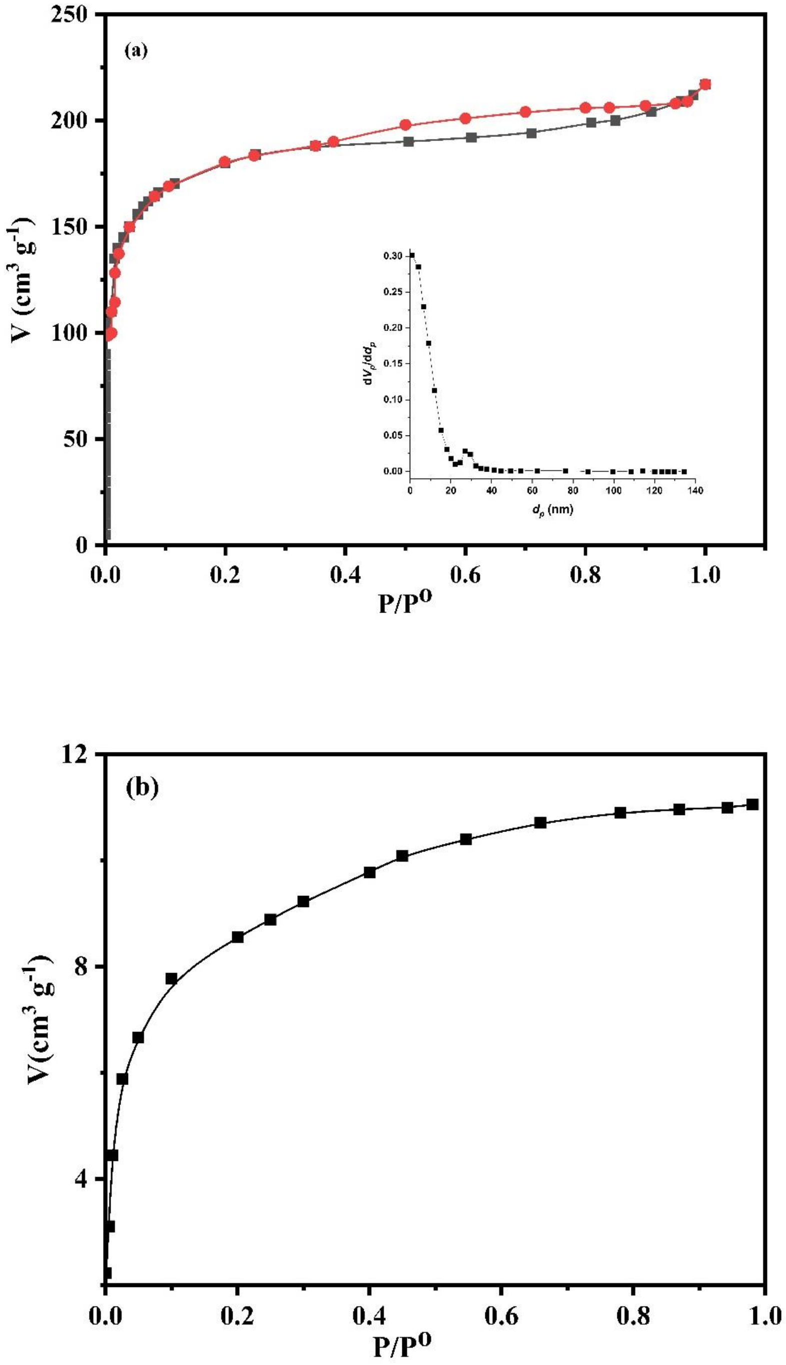

Figure 4. Nitrogen gas adsorption/desorption isotherm for (**a**) the activated carbon sample (inserted BJH plot) and (**b**) the native rice husk at −196 °C.

2.2. *Optimization of Removal Conditions*

2.2.1. Effect of Initial pH of the Solution

One of the significant factors influencing the adsorption and removal of pollutants from aqueous solutions is initial pH [39]. The impact of pH on the removal of COD was investigated at a range of 2.0–8.0. As shown in Figure 5, the uptake of COD is effective at a pH ranged from 3.0 to 5.0; then, it decreases again after that. At this pH range, the surface of the activated carbon becomes positive due to the accumulation of hydronium ions and therefore can bind to negatively charged organic species by electrostatic attraction [40]. In contrast, at higher pH, the adsorbed hydroxyl ions compete with the organic species for the active sites on the active carbon surface, causing a significant reduction in the removal of both COD [41]. Based on these findings, pH 3.0 was selected for further experiments.

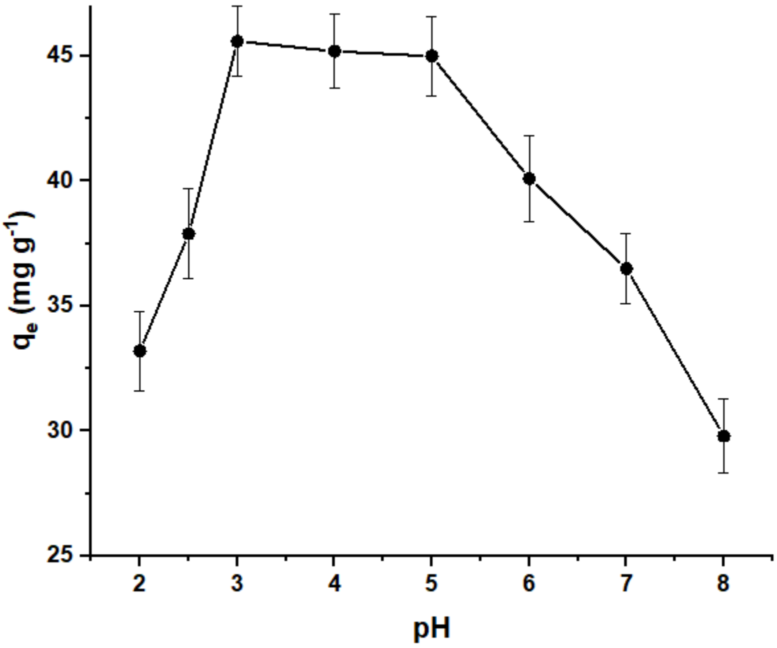

Figure 5. Effect of pH on the removal of COD by the activated carbon.

2.2.2. Effect of Active Carbon Dose

The effectiveness of COD removal is shown in Figure 6 as a function of adsorbent dosage. The adsorbent dosages were adjusted to range from 0.5 to 2.0 g L^{-1}. As we can clearly see, the uptake increases by increasing the sorbent dose due to the increased adsorbent surface area and the number of accessible adsorption sites. The maximum adsorption was achieved at 0.1 g L^{-1}, and the removal was not enhanced significantly by increasing the dose of sorbent beyond this limit. Therefore, a sorbent amount of 0.1 g L^{-1} was taken as the optimum value during the study.

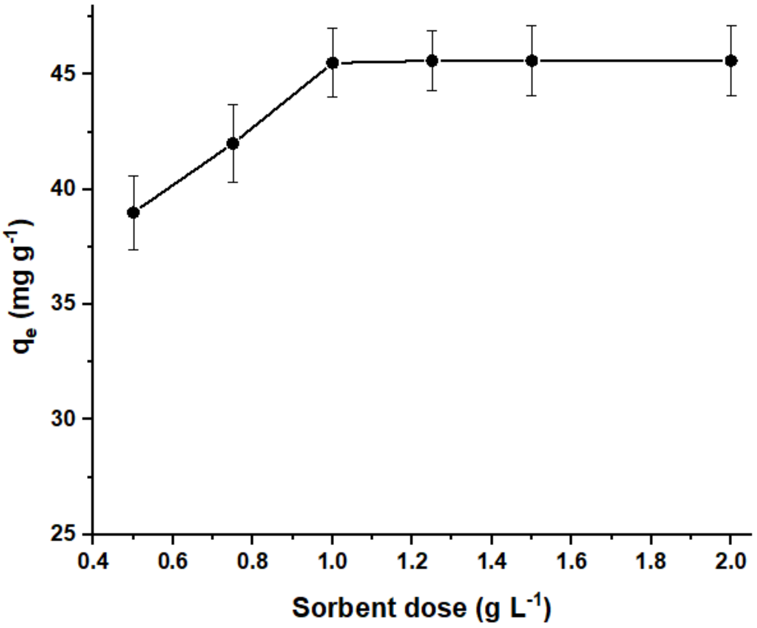

Figure 6. Effect of sorbent dose on the removal of COD by the activated carbon.

2.2.3. Effect of Shaking Time

The impact of shaking time on the adsorption of COD by the activated carbon was investigated at time intervals from 30 to 150 min at a fixed shaking rate (200 rpm). As presented in Figure 7, the removal of COD increases with shaking time and reaches a plateau at 100 min. Increased time, up to 100 min, results in increased contact between the solution and the adsorption sites on the sorbent surface, and therefore, the removal rate is rapid. As the contact time passed, the adsorbent sites tended to become saturated. As a result, all subsequent experiments employed a contact time of 100 min.

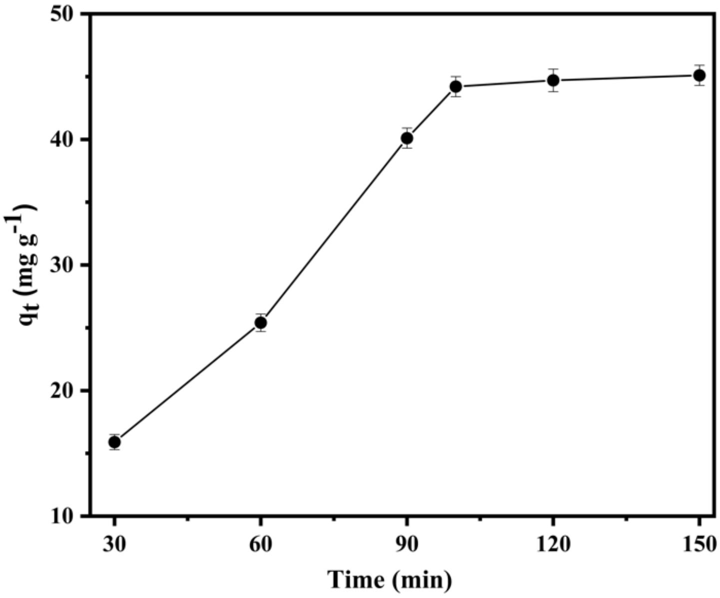

Figure 7. Effect of shaking time on the removal of COD by the activated carbon.

2.2.4. Effect of Temperature

The influence of temperature on COD adsorption was studied at temperatures ranging from 25 to 50 °C. The results shown in Figure 8 show that increasing the temperature gradually decreases the removal of COD by the activated carbon. As can be seen, the increase in temperature from 25 to 50 °C reduces COD sorption efficiency from 97.0 to 74.5%. This behavior indicates that the adsorption process is exothermic.

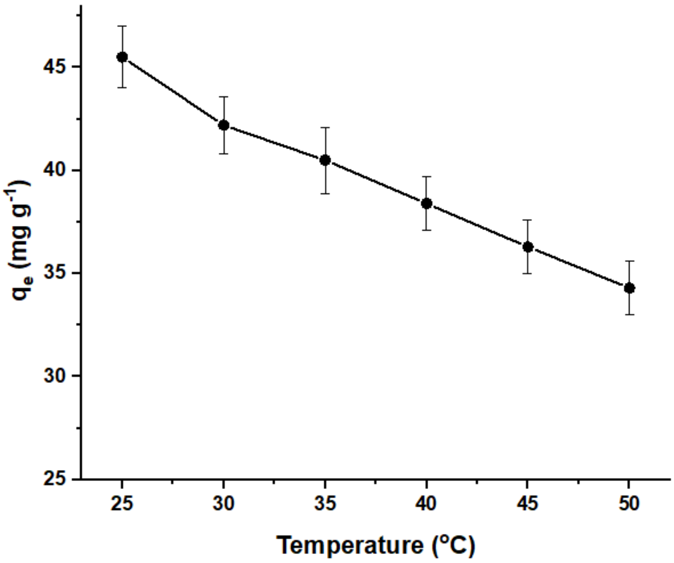

Figure 8. Effect of temperature on the removal of COD by activated carbon.

2.2.5. Adsorption Isotherm

The Langmuir model was utilized in this study to investigate the equilibrium characteristics of COD removal. According to the Langmuir model, adsorption takes place at specific homogenous sites on the adsorbent's surface, and the energy level distribution is constant. The Langmuir isotherm can be stated mathematically as:

$$\frac{C_e}{q_e} = \frac{C_e}{q_{max}} + \frac{1}{q_{max}K_L} \tag{1}$$

where q_{max} is the maximum adsorption capacity (mg g^{-1}) and K_L is the Langmuir constant.

By plotting C_e versus C_e/q_e (Figure 9), a linear relation (R^2 = 0.9942) was achieved, suggesting that the model is appropriate to explain the adsorption of COD by the activated carbon. Moreover, the relation can be used to estimate the maximum adsorption capacity (q_{max}), which was 45.9 mg g^{-1}.

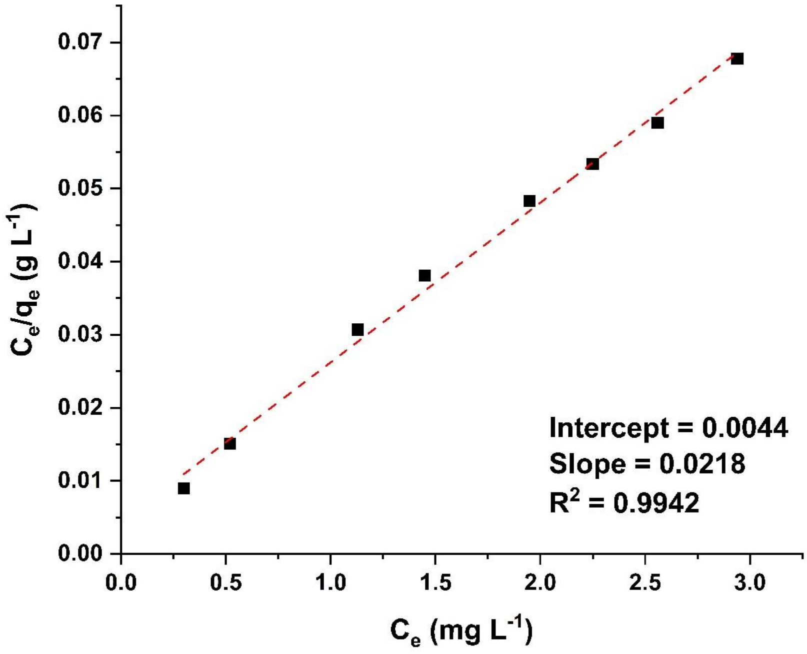

Figure 9. Langmuir adsorption isotherm of COD by activated carbon.

2.2.6. Kinetic Studies

The rate and mechanism of COD adsorption onto the studied solid adsorbents were studied using pseudo-first (PFO, Equation (2)) and pseudo-second (PSO, Equation (3)) order kinetic models.

$$\ln(q_e - q_t) = \ln(q_e) - k_1 t \tag{2}$$

$$\frac{t}{q_t} = \frac{1}{k_2 {q_e}^2} + \frac{t}{q_e} \tag{3}$$

Herein, q_e and q_t (mg g^{-1}) are the amounts of COD adsorbed at equilibrium and at time t (min), respectively, and they were calculated from Equation (1); k_1 (min^{-1}) and k_2 (g mg^{-1} min^{-1}) are PFO and PSO rate constants, respectively. Meanwhile, C_t (mg L^{-1}) is the equilibrium concentration of COD at time t (min).

The PFO and PSO kinetic models are presented in Figure 10a,b, respectively. The calculated kinetic parameters from the PFO kinetic models confirm that the adsorption of COD onto the prepared activated carbon sample follows PFO. The calculated correlation coefficient (R^2), first-order rate constant, and the experimental adsorption capacity are found to be 0.9792, 0.01921 min^{-1}, and 46.3 mg g^{-1}, respectively. The higher R^2 value and the smaller difference between the Langmuir maximum adsorption capacity (q_m, 45.9 mg g^{-1})

and that calculated using PFO (q_{exp}, 46.3 mg g^{-1}) prove the sufficient application of the PFO model. Applying the PSO model, we found that the R^2 value is very low (0.76508), and the calculated q_{exp} (105.8 mg g^{-1}) using PSO is largely different from that calculated from the Langmuir model.

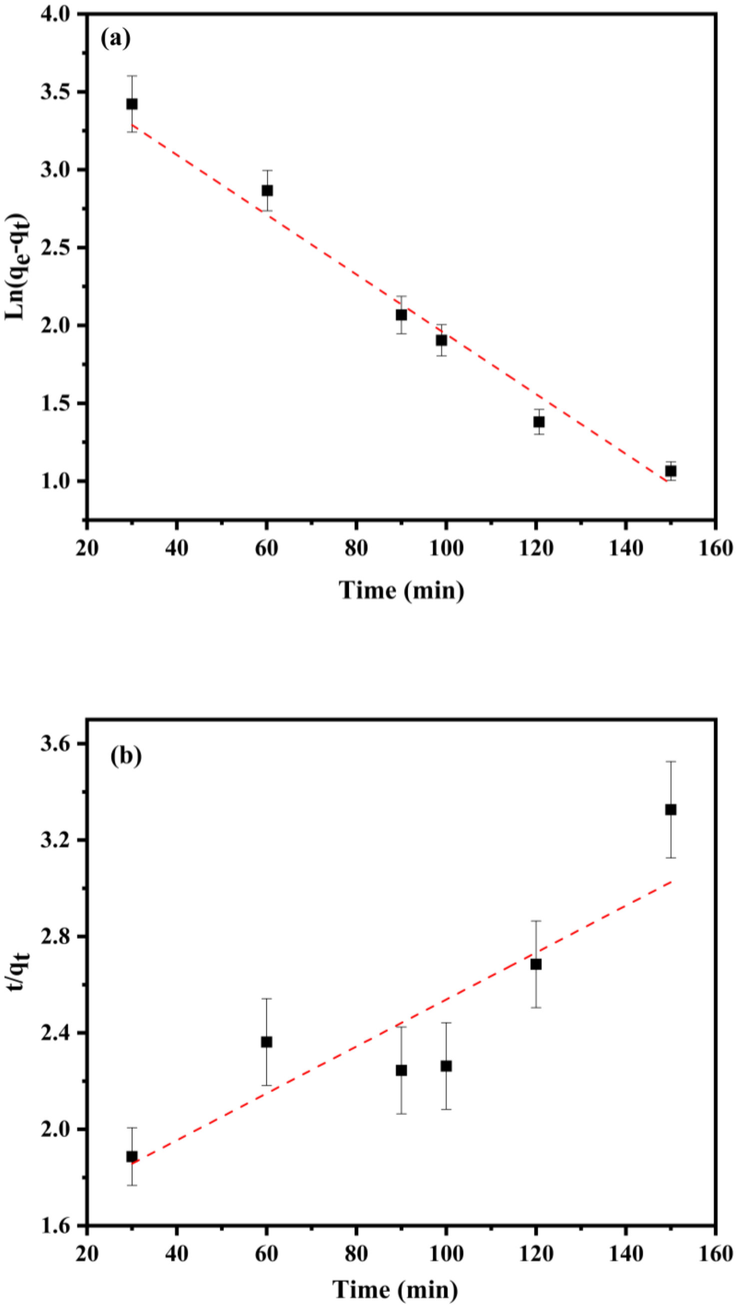

Figure 10. (**a**) Pseudo-first order and (**b**) Pseudo-second-order adsorption kinetics of COD onto the prepared activated carbon.

2.2.7. Comparison of COD Adsorption Efficiencies with Various Adsorbents

Table 1 compares the adsorption capacity and the surface area of the prepared active carbon and those of various adsorbents. When compared to some previous studies reported in the literature, the active carbon prepared in this study demonstrated comparable and relatively better efficiency in removing COD due to its higher surface area.

Table 1. Comparison of surface area and adsorption capacity of various adsorbents.

Adsorbent	Surface Area (m^2 g^{-1})	Adsorption Capacity (mg g^{-1})	Reference
Tea waste biochar	60.0	12.0	[42]
Zeolite–carbon composite	60.9	4.5	[43]
Fe_2O_3 nanoparticles	-	21.3	[44]
Activated carbon prepared from animal horns	-	6.5	[45]
Granular activated carbon	719.5	13.3	[46]
Chemically activated carbon from rice husk	813.5	45.9	Our study

3. Material and Methods

3.1. Chemicals

In this study, analytical grade reagents and chemicals from Sigma-Aldrich (St. Loius, MO, USA) were used. Double-distilled water was used for the preparation of aqueous solutions and dilution. The wastewater samples were collected in 2.0 L polypropylene containers from Kitchener drain at Kafr El-Sheikh Governorate, Egypt. The samples were transported to the laboratory in an icebox and kept in a refrigerator at 4 °C. Table 2 displays the initial characteristic features of the pre-treated wastewater samples.

Table 2. Initial characterization of wastewater samples.

Parameter	Value
Temperature	22.5 °C
pH	7.8
Electric conductivity	1.3 dsm^{-1}
COD	200 mg L^{-1}
Ammonia	19.2 mg L^{-1}
Nitrate	19.7 mg L^{-1}
Phosphate	0.67 mg L^{-1}
Total solids	3360 mg L^{-1}
Total suspended solids	1940 mg L^{-1}
Total dissolved solids	1420 mg L^{-1}

3.2. Preparation of Active Carbon from Rice Husk

Raw rice husks were obtained from a rice mill in Mansoura City, Egypt. A sample of rice husks (about 50 g) was rinsed with distilled water to eliminate dust and other contaminants before being dried at 90 °C for 24 h. About 30 g of the dried sample was soaked for 48 h in 100 mL of distilled water containing 60 g of $ZnCl_2$. After that, the mixture was dried at 90 °C until a constant weight is reached. The obtained mass was ground and ignited in a stainless steel tube under nitrogen atmosphere at 600 °C (Hydrogen Furnace (BR-16AH2-5) brother furnace, China). The obtained activated carbon was washed with distilled water and dried at 90 °C for 24 h.

3.3. Characterization of Activated Carbon

The prepared activated carbon was characterized by Fourier transform infrared spectra (FT-IR) recorded on a KBr disc on a Thermo-Nicolet IS10 FT-IR spectrometer (Nicolet Instrument Co., Madison, WI, USA), scan electron microscope (SEM) (Hitachi SX-650, Tokyo, 180 Japan) and Brunauer–Emmet–Teller analysis (BET). High magnification micrographs of the prepared samples were obtained using high-resolution transmission electron microscopy (TEM) (JEOL 2100F TEM). The apparatus was run at a 200 kV accelerating voltage. After 30 min of ultrasonic treatment in ethanol, the sample was deposited onto a Cu TEM grid that had been coated with carbon. The generated chemically activated carbon's textural characteristics, including pore radius ($\bar{r}$, nm), total pore volume (V_T, cm^3

g^{-1}), and specific surface area (S_{BET}, $m^2\ g^{-1}$), were examined by nitrogen gas adsorption using a NOVA3200e gas sorption analyzer (Quantachrome Instruments, Florida, USA). The tested samples underwent a 24 h degassing process at 105 Torr and 150 °C.

3.4. Batch Adsorption Tests with Activated Carbon for COD Removal

COD were determined before and after treatment with activated carbon by a photometric Lovibond apparatus (Set-Up MD 100). The analyses were carried out in the Soil Fertility and Fertilizers Quality Control Laboratory of the Faculty of Agriculture, Mansoura University certified by the Egyptian Accreditation Council (EGAC) and recognized in ISO/IEC 17,025. All the tests were carried out in batch mode at room temperature. Briefly, 100 mL of water sample of initial COD = C_i was stirred for 100 min at 200 rpm with 100 mg of the activated carbon at pH 3.0. After that, the activated carbon was removed by filtration, and the concentration of COD was determined in the supernatant at equilibrium (C_f). The adsorption capacity (q_e) was calculated by Equation (4):

$$q_e\left(\mathrm{mg\ g^{-1}}\right) = \frac{(C_i - C_e)V}{m} \tag{4}$$

where V is the initial volume of solution (L), and m is the mass of active carbon (g).

4. Conclusions

The present work showed that the chemically activated carbon prepared from rice husk is effective for the elimination of COD from wastewater. The adsorption process was found to be impacted by pH, contact time, dose of sorbent and temperature. The adsorption equilibrium was achieved in 100 min. The adsorption data fit well to the Langmuir adsorption model with a maximum adsorption capacity of 45.9 mg g^{-1}. Owing to its high surface area, porosity and availability, activated carbon from agriculture wastes can be applied at a large scale to remove different pollutants from wastewater. Finally, converting discarded rice husk into activated carbons with excellent adsorptive features assists the environment greatly. Accordingly, manufactured low-cost adsorbents have the potential to be used in water purification while avoiding the requirement for landfilling.

Author Contributions: All authors contributed to the study conception and design. Material preparation, data collection and analysis were performed by W.I.M., R.A.M., A.A.A.M., M.M.A. and A.F.H. The first draft of the manuscript was written by W.I.M., R.A.M., A.A.A.M., M.M.A. All authors commented on previous versions of the manuscript. All authors have read and agreed to the published version of the manuscript.

Funding: The authors declare that no funds, grants, or other support were received during the preparation of this manuscript.

Institutional Review Board Statement: Not applicable.

Informed Consent Statement: Not applicable.

Data Availability Statement: Not applicable.

Conflicts of Interest: The authors declare no conflict of interest.

References

1. Burian, S.; Walsh, T.; Kalyanapu, A.; Larsen, S. 5.06-Climate Vulnerabilities and Adaptation of Urban Water Infrastructure Systems. In *Climate Vulnerability*; Academic Press: Oxford, UK, 2013; pp. 87–107.
2. Saxena, G.; Chandra, R.; Bharagava, R.N. Environmental pollution, toxicity profile and treatment approaches for tannery wastewater and its chemical pollutants. *Rev. Environ. Contam. Toxicol.* **2016**, *240*, 31–69.
3. Abdalla, K.Z.; Hammam, G. Correlation between biochemical oxygen demand and chemical oxygen demand for various wastewater treatment plants in Egypt to obtain the biodegradability indices. *Int. J. Sci. Basic Appl. Res.* **2014**, *13*, 42–48.
4. Geerdink, R.B.; van den Hurk, R.S.; Epema, O.J. Chemical oxygen demand: Historical perspectives and future challenges. *Anal. Chim. Acta* **2017**, *961*, 1–11. [CrossRef]

5. Lv, Z.; Xiao, X.; Wang, Y.; Zhang, Y.; Jiao, N. Improved water quality monitoring indicators may increase carbon storage in the oceans. *Environ. Res.* **2022**, *206*, 112608. [CrossRef]
6. Alipour, Z.; Azari, A. COD removal from industrial spent caustic wastewater: A review. *J. Environ. Chem. Eng.* **2020**, *8*, 103678. [CrossRef]
7. Bote, M.E. Studies on electrode combination for COD removal from domestic wastewater using electrocoagulation. *Heliyon* **2021**, *7*, e08614. [CrossRef]
8. Ilhan, F.; Ulucan-Altuntas, K.; Dogan, C.; Kurt, U. Treatability of raw textile wastewater using Fenton process and its comparison with chemical coagulation. *Desalin. Water Treat.* **2019**, *162*, 142–148. [CrossRef]
9. Pijarn, N.; Intaraprasert, J.; Ophap, S.; Uma, T.; Deekarnkol, S.; Bowornkietkaew, W. Microstructural characterization of white charcoal for rapid reduction of chemical oxygen demand and automatically adjust pH to neutral in wastewater treatment. *J. Mater. Res. Technol.* **2021**, *13*, 336–345. [CrossRef]
10. Alhweij, H.; Emanuelsson, E.A.C.; Shahid, S.; Wenk, J. Organic matter removal and antifouling performance of sulfonated polyaniline nanofiltration (S-PANI NF) membranes. *J. Environ. Chem. Eng.* **2022**, *10*, 107906. [CrossRef]
11. Zhou, L.; Wang, S.; Li, Z.; Cao, X.; Liu, R.; Yun, J. Simultaneously removal of phosphorous and COD for purification of organophosphorus wastewater by catalytic ozonation over CaO. *J. Water Process Eng.* **2023**, *51*, 103397. [CrossRef]
12. Tan, Y.-J.; Sun, L.-J.; Li, B.-T.; Zhao, X.-H.; Yu, T.; Ikuno, N.; Ishii, K.; Hu, H.-Y. Fouling characteristics and fouling control of reverse osmosis membranes for desalination of dyeing wastewater with high chemical oxygen demand. *Desalination* **2017**, *419*, 1–7. [CrossRef]
13. Crini, G.; Lichtfouse, E. Advantages and disadvantages of techniques used for wastewater treatment. *Environ. Chem. Lett.* **2019**, *17*, 145–155. [CrossRef]
14. Gutiérrez, M.; Grillini, V.; Pavlović, D.M.; Verlicchi, P. Activated carbon coupled with advanced biological wastewater treatment: A review of the enhancement in micropollutant removal. *Sci. Total Environ.* **2021**, *790*, 148050. [CrossRef]
15. Karić, N.; Maia, A.S.; Teodorović, A.; Atanasova, N.; Langergraber, G.; Crini, G.; Ribeiro, A.R.; Đolić, M. Bio-waste valorisation: Agricultural wastes as biosorbents for removal of (in) organic pollutants in wastewater treatment. *Chem. Eng. J. Adv.* **2022**, *9*, 100239. [CrossRef]
16. Wong, S.; Ngadi, N.; Inuwa, I.M.; Hassan, O. Recent advances in applications of activated carbon from biowaste for wastewater treatment: A short review. *J. Clean. Prod.* **2018**, *175*, 361–375. [CrossRef]
17. Laksaci, H.; Belhamdi, B.; Khelifi, O.; Khelifi, A.; Trari, M. Elimination of amoxicillin by adsorption on coffee waste based activated carbon. *J. Mol. Struct.* **2023**, *1274*, 134500. [CrossRef]
18. Ugwu, E.I.; Agunwamba, J.C. A review on the applicability of activated carbon derived from plant biomass in adsorption of chromium, copper, and zinc from industrial wastewater. *Environ. Monit. Assess.* **2020**, *192*, 240. [CrossRef]
19. Xiao, W.; Garba, Z.N.; Sun, S.; Lawan, I.; Wang, L.; Lin, M.; Yuan, Z. Preparation and evaluation of an effective activated carbon from white sugar for the adsorption of rhodamine B dye. *J. Clean. Prod.* **2020**, *253*, 119989. [CrossRef]
20. Januário, E.F.D.; Fachina, Y.J.; Wernke, G.; Demiti, G.M.M.; Beltran, L.B.; Bergamasco, R.; Vieira, A.M.S. Application of activated carbon functionalized with graphene oxide for efficient removal of COVID-19 treatment-related pharmaceuticals from water. *Chemosphere* **2022**, *289*, 133213. [CrossRef]
21. Boumaraf, R.; Khettaf, S.; Benmahdi, F.; Bouzzafa, M.; Bouhidel, K.-E.; Bouhelassa, M. Removal of the neutral dissolved organic matter from surface waters by activated carbon. *Arab. J. Geosci.* **2022**, *15*, 151. [CrossRef]
22. Li, G.; Li, J.; Tan, W.; Yang, M.; Wang, H.; Wang, X. Effectiveness and mechanisms of the adsorption of carbendazim from wastewater onto commercial activated carbon. *Chemosphere* **2022**, *304*, 135231. [CrossRef]
23. Shao, Y.; Li, J.; Fang, X.; Yang, Z.; Qu, Y.; Yang, M.; Tan, W.; Li, G.; Wang, H. Chemical modification of bamboo activated carbon surface and its adsorption property of simultaneous removal of phosphate and nitrate. *Chemosphere* **2022**, *287*, 132118. [CrossRef]
24. Yunus, Z.M.; Al-Gheethi, A.; Othman, N.; Hamdan, R.; Ruslan, N.N. Advanced methods for activated carbon from agriculture wastes; a comprehensive review. *Int. J. Environ. Anal. Chem.* **2022**, *102*, 134–158. [CrossRef]
25. Masoud, M.S.; El-Saraf, W.M.; Abdel-Halim, A.M.; Ali, A.E.; Mohamed, E.A.; Hasan, H.M. Rice husk and activated carbon for waste water treatment of El-Mex Bay, Alexandria Coast, Egypt. *Arab. J. Chem.* **2016**, *9*, S1590–S1596. [CrossRef]
26. Oliver, S.P.; Jayarao, B.M.; Almeida, R.A. Foodborne pathogens in milk and the dairy farm environment: Food safety and public health implications. *Foodbourne Pathog. Dis.* **2005**, *2*, 115–129. [CrossRef]
27. Afroze, S.; Sen, T.K. A review on heavy metal ions and dye adsorption from water by agricultural solid waste adsorbents. *Water Air Soil Pollut.* **2018**, *229*, 225. [CrossRef]
28. Spagnoli, A.A.; Giannakoudakis, D.A.; Bashkova, S. Adsorption of methylene blue on cashew nut shell based carbons activated with zinc chloride: The role of surface and structural parameters. *J. Mol. Liq.* **2017**, *229*, 465–471. [CrossRef]
29. Demiral, H.; Demiral, İ. Surface properties of activated carbon prepared from wastes. *Surf. Interface Anal. Int. J. Devoted Dev. Appl. Tech. Anal. Surf. Interfaces Thin Film.* **2008**, *40*, 612–615. [CrossRef]
30. Nahil, M.A.; Williams, P.T. Characterisation of activated carbons with high surface area and variable porosity produced from agricultural cotton waste by chemical activation and co-activation. *Waste Biomass Valorization* **2012**, *3*, 117–130. [CrossRef]
31. Rivas, A.; Vera, G.; Palacios, V.; Rigail, A.; Cornejo Martínez, M. Characterization of Rice Husk and the Crystallization Process of Amorphous Silica from Rice Husk Ash. In Proceedings of the 14th LACCEI International Multi-Conference for Engineering, Education, and Technology: Engineering Innovations for Global Sustainability, San José, CA, USA, 20–22 July 2016; pp. 1–9.

32. Ketcome, N.; Grisdanurak, N.; Chiarakorn, S. Silylated rice husk MCM-41 and its binary adsorption of water–toluene mixture. *J. Porous Mater.* **2009**, *16*, 41–46. [CrossRef]
33. Nabieh, K.A.; Mortada, W.I.; Helmy, T.E.; Kenawy, I.M.; Abou El-Reash, Y.G. Chemically modified rice husk as an effective adsorbent for removal of palladium ions. *Heliyon* **2021**, *7*, e06062. [CrossRef]
34. Yu, H.-M.; Song, H.; Chen, M.-L. Dithizone immobilized silica gel on-line preconcentration of trace copper with detection by flame atomic absorption spectrometry. *Talanta* **2011**, *85*, 625–630. [CrossRef] [PubMed]
35. Mortada, W.I.; Nabieh, K.A.; Helmy, T.E.; Abou El-Reash, Y.G. Microwave-assisted synthesis of MCM-41 composite with rice husk and its functionalization by dithizone for preconcentration of some metal ions from water and food samples. *J. Food Compos. Anal.* **2022**, *106*, 104352. [CrossRef]
36. Ahiduzzaman, M.; Sadrul Islam, A. Preparation of porous bio-char and activated carbon from rice husk by leaching ash and chemical activation. *SpringerPlus* **2016**, *5*, 1248. [CrossRef] [PubMed]
37. Lester, E.; Hilal, N.; Henderson, J. Porosity in ancient glass from Syria (c. 800 AD) using gas adsorption and atomic force microscopy. *Surf. Interface Anal. Int. J. Devoted Dev. Appl. Tech. Anal. Surf. Interfaces Thin Film.* **2004**, *36*, 1323–1329.
38. ALOthman, Z.A. A review: Fundamental aspects of silicate mesoporous materials. *Materials* **2012**, *5*, 2874–2902. [CrossRef]
39. Mortada, W.I.; Abdelghany, A.M. Preconcentration of lead in blood and urine samples among bladder cancer patients using mesoporous strontium titanate nanoparticles. *Biol. Trace Elem. Res.* **2020**, *193*, 100–110. [CrossRef]
40. Lokeshwari, N.; Joshi, K. Low cost adsorbent for reducing organic components. *I Control. Pollut.* **2014**, *30*, 53–58.
41. Nayl, A.E.A.; Elkhashab, R.A.; El Malah, T.; Yakout, S.M.; El-Khateeb, M.A.; Ali, M.; Ali, H.M. Adsorption studies on the removal of COD and BOD from treated sewage using activated carbon prepared from date palm waste. *Environ. Sci. Pollut. Res.* **2017**, *24*, 22284–22293. [CrossRef]
42. Khurshid, H.; Mustafa, M.R.U.; Rashid, U.; Isa, M.H.; Ho, Y.C.; Shah, M.M. Adsorptive removal of COD from produced water using tea waste biochar. *Environ. Technol. Innov.* **2021**, *23*, 101563. [CrossRef]
43. Halim, A.A.; Aziz, H.A.; Johari, M.A.M.; Ariffin, K.S.; Adlan, M.N. Ammoniacal nitrogen and COD removal from semi-aerobic landfill leachate using a composite adsorbent: Fixed bed column adsorption performance. *J. Hazard. Mater.* **2010**, *175*, 960–964. [CrossRef] [PubMed]
44. Nassar, N.N.; Arar, L.A.; Marei, N.N.; Ghanim, M.M.A.; Dwekat, M.S.; Sawalha, S.H. Treatment of olive mill based wastewater by means of magnetic nanoparticles: Decolourization, dephenolization and COD removal. *Environ. Nanotechnol. Monit. Manag.* **2014**, *1*, 14–23. [CrossRef]
45. Emmanuel, O.A.; Olalekan, A.B. COD removal from industrial wastewater using activated carbon prepared from animal horns. *Afr. J. Biotechnol.* **2008**, *7*, 3887–3891.
46. Mohammad-Pajooh, E.; Turcios, A.E.; Cuff, G.; Weichgrebe, D.; Rosenwinkel, K.-H.; Vedenyapina, M.; Sharifullina, L. Removal of inert COD and trace metals from stabilized landfill leachate by granular activated carbon (GAC) adsorption. *J. Environ. Manag.* **2018**, *228*, 189–196. [CrossRef] [PubMed]

Disclaimer/Publisher's Note: The statements, opinions and data contained in all publications are solely those of the individual author(s) and contributor(s) and not of MDPI and/or the editor(s). MDPI and/or the editor(s) disclaim responsibility for any injury to people or property resulting from any ideas, methods, instructions or products referred to in the content.